Transition states and thermal collapse of dipolar Bose-Einstein condensates

Andrej Junginger,* Manuel Kreibich, Jörg Main, and Günter Wunner

Institut für Theoretische Physik 1, Universität Stuttgart, 70550 Stuttgart, Germany

(Dated: September 19, 2018)

We investigate thermally excited, dipolar Bose-Einstein condensates. Quasi-particle excitations of the atomic cloud cause density fluctuations which can induce the collapse of the condensate if the inter-particle interaction is attractive. Within a variational approach, we identify the collectively excited stationary states of the gas which form transition states on the way to the BEC's collapse. We analyze transition states with different m-fold rotational symmetry and identify the one which mediates the collapse. The latter's symmetry depends on the trap aspect ratio of the external trapping potential which determines the shape of the BEC. Moreover, we present the collapse dynamics of the BEC and calculate the corresponding decay rate using transition state theory. We observe that the thermally induced collapse mechanism is important near the critical scattering length, where the lifetime of the condensate can be significantly reduced. Our results are valid for an arbitrary strength of the dipole-dipole interaction. Specific applications are discussed for the elements ^{52}Cr, ^{164}Dy and ^{168}Er with which dipolar BECs have been experimentally realized.

I. INTRODUCTION

The Bose-Einstein condensation of atoms with considerable magnetic dipole moment such as ^{52}Cr, ^{164}Dy and ^{168}Er atoms [1–3] has opened new perspectives in the field of ultra-cold quantum gases. Due to their electronic structure, these atoms exhibit magnetic moments of several Bohr magnetons, so that the bosons interact significantly via the long-range and anisotropic dipole-dipole interaction (DDI) in addition to the occurrence of scattering processes. As a consequence of the anisotropic DDI, a wealth of new phenomena emerges in dipolar Bose-Einstein condensates (BECs). These include isotropic as well as anisotropic solitons [4–6], biconcave or structured ground state density distributions [7–9], stability diagrams that crucially depend on the trap geometry [10–12], radial and angular rotons [8, 13, 14], and anisotropic collapse dynamics [15, 16].

An important issue in the field of ultra-cold quantum gases is the stability of the gas. A BEC is a metastable state and several mechanisms can contribute to its decay, e. g. inelastic three-body collisions, dipolar relaxation [17], macroscopic quantum tunneling [18, 19], or the decrease of the s-wave scattering length below its critical value [8]. Another decay mechanism is the coherent collapse of the atomic cloud due to thermal excitations. This process is based on the fact that quasi-particle excitations in an excited BEC lead to time-dependent density fluctuations of the gas. If the inter-particle interaction is attractive, these fluctuations can induce the collapse of the condensate, when the density locally becomes high enough so that the attraction cannot be compensated anymore by the quantum pressure. This process is important near the critical scattering length where the attraction between the bosons becomes dominant. Hints to

a thermally induced collapse can be found in the experiment by Koch *et al.* [10]. They measured the value of the critical scattering length and, for a wide range of the trap aspect ratio, they obtained values which were larger than predicted in their theoretical investigations.

In a recent publication [20] we have shown qualitatively within a simple variational approach that the thermally induced collapse of dipolar BECs is fascinating, because the collapse dynamics can – depending on the external physical parameters – break the symmetry of the confining trap. In this paper we present investigations of a thermally excited dipolar BEC within an *extended* variational approach. Far beyond our previous investigations using a single Gaussian trial wave function [20] the extended approach is capable to also reproduce the biconcave shape of the ground state wave function occurring for certain trapping parameters [21] and to describe complex dynamics of the dipolar BEC. The latter include the local collapse or collective oscillations and elementary excitations with arbitrary m-fold rotational symmetry [22]. Moreover, stability analyses [21, 22] within the extended approach have revealed qualitative differences as compared to the single Gaussian ansatz: A pitchfork bifurcation of the BEC's ground state is responsible for the instability of the dipolar BEC below a certain value of the scattering length and a whole cascade of bifurcations occurs when the scattering length is further decreased. The occurrence of these bifurcations gives rise to the expectation that, in addition to its ground state, further (unstable) stationary states exist in dipolar BECs and that it is exactly these states which form the transition states of the condensate on the way to its collapse.

For our investigations, we consider temperatures T in the region $0 < T_0 < T \ll T_c$. Below a temperature T_0, collective oscillations of the BEC are not thermally excited and macroscopic quantum tunneling will be the dominant decay mechanism. At $T > T_0$, the collective dynamics of the condensate is excited, and above T_c the

BEC does not exist anymore. At temperatures $T \ll T_c$ small compared to the critical one, the condensate is almost pure and excitations of single bosons to higher quantum states can be neglected, so that the condensate can be described in a mean-field approximation by the Gross-Pitaevskii equation (GPE). At temperatures which are on the order of the critical temperature, $T \approx T_c$, a significant number of bosons will occupy excited states and Hartree-Fock-Bogoliubov theory [23, 24] can be applied. Also c-field methods [25] allow for the investigation of the finite-temperature BEC up to the critical temperature when the contribution of incoherent particles in the gas is of importance. This regime is, however, not subject of our investigations.

Our paper is organized as follows: In Sec. II, we present the theoretical description of the dipolar BEC within the framework of the GPE and introduce particle number scaled units. Moreover, the variational approach to the condensate's wave function as well as the calculation of the thermal decay rate by applying transition state theory (TST) is demonstrated. The results are presented in Sec. III. Here we discuss the presence of various transition states with different m-fold rotational symmetry, the dynamics of BECs which are excited above the corresponding activation energy and the decay rate of the condensate. Our results are valid for an arbitrary strength of the dipole-dipole interaction and, at the end of Sec. III, we discuss applications to the elements ^{52}Cr, ^{164}Dy and ^{168}Er which possess different magnetic moments.

II. THEORY

A. The dipolar BEC

If the temperature of the quantum gas is small compared to the critical temperature T_c, then excitations of single bosons to higher quantum states can be neglected and the atomic cloud can be described by a single order parameter $\psi(\mathbf{r},t)$ which is a solution of the time-dependent GPE

$$\begin{aligned} i\partial_t \psi(\mathbf{r},t) &= \hat{H}\psi(\mathbf{r},t) \\ &= \left(-\Delta + V_{\text{ext}} + V_{\text{int}}\right)\psi(\mathbf{r},t). \end{aligned} \quad (1)$$

Here, the terms V_{ext} and V_{int} describe the interactions of the bosons with an external trapping potential as well as the inter-particle interaction,

$$V_{\text{ext}} = \gamma_\rho^2 \rho^2 \left[1 + s\cos(m\phi)\right] + \gamma_z^2 z^2, \quad (2)$$

$$\begin{aligned} V_{\text{int}} = &8\pi a \left|\psi(\mathbf{r},t)\right|^2 \\ &+ \int d^3\mathbf{r}' \frac{1 - 3\cos^2\theta}{|\mathbf{r} - \mathbf{r}'|^3} \left|\psi(\mathbf{r}',t)\right|^2. \end{aligned} \quad (3)$$

In Eq. (2), $\gamma_{\rho,z}$ denote the strength of the external trapping potential which is harmonic in both the radial and z-direction and cylindrically symmetric for $s = 0$. For $s \neq 0$, this symmetry can be broken in a way that the trap exhibits an m-fold rotational symmetry. However, note that we always investigate condensates in axisymmetric traps ($s = 0$) in this paper and that the additional term for $s \neq 0$ is only used to specifically access the excited states as discussed in the appendix. The inter-particle interaction V_{int} on the one hand takes into account low-energy scattering processes between two bosons which are described by the s-wave scattering length a. On the other hand, it describes the long-range DDI between the bosons which we assume to be aligned along the z-direction by an external magnetic field (θ is the angle between the z-axis and the vector $\mathbf{r} - \mathbf{r}'$).

The GPE (1) and the interaction terms (2)–(3) are given in dimensionless units which we obtained by measuring lengths in terms of the "dipole length" $a_d = m\mu_0\mu^2/(2\pi\hbar^2)$, energies in units of $E_d = \hbar^2/(2ma_d^2)$, frequencies in terms of $\omega_d = E_d/\hbar$ and inverse temperatures in multiples of $\beta_d = E_d^{-1}$. Furthermore, we applied a particle number scaling

$$(\mathbf{r}, \psi, E, \beta, \omega) \longrightarrow (N\mathbf{r}, N^{-3/2}\psi, N^{-1}E, N\beta, N^{-2}\omega) \quad (4)$$

in order to eliminate the explicit occurrence of the particle number N in the interaction terms and define the trapping parameters as $\gamma_{\rho,z} = \omega_{\rho,z}/(2N^2\omega_d)$ where $\omega_{\rho,z}$ are the trap frequencies in SI units.

B. Variational approach to the GPE

1. The time-dependent variational principle

There are several ways to solve the GPE (1), one of which is the discretization of the wave function on grids. The dynamics can then be calculated using the split-operator method and the ground state of the BEC is accessible via an imaginary time evolution of Eq. (1).

For our purpose, a more powerful approach is the solution of the GPE within a variational framework, because this allows to access collectively excited stationary states of the GPE which play a crucial role in our investigation. In this variational approach, the time-dependent wave function $\psi(\mathbf{r},t) = \psi(\mathbf{r}, \mathbf{z}(t))$ describing the BEC is expressed in terms of a set of time-dependent and complex variational parameters $\mathbf{z}(t)$. An approximate solution of the GPE in the Hilbert subspace spanned by the variational parameters is then given by the McLachlan variational principle [26]. This claims the norm of the difference between the left- and the right-hand side of the GPE to be minimal, i.e.

$$\|i\dot{\psi} - \hat{H}\psi\| \overset{!}{=} \min, \quad (5)$$

where the variation is carried out with respect to $\dot{\psi}$ (for simplicity, we have omitted the arguments $(\mathbf{r},t)$ of the wave function). Applying this variational principle to a parameterized wave function $\psi(\mathbf{r}, \mathbf{z}(t))$, one obtains the

set of ordinary first order differential equations [27]

$$\left\langle \frac{\partial \psi}{\partial z} \middle| \frac{\partial \psi}{\partial z} \right\rangle \dot{z} = -\mathrm{i} \left\langle \frac{\partial \psi}{\partial z} \middle| \hat{H} \middle| \psi \right\rangle \qquad (6)$$

which determine the time evolution of the wave function. The mean-field energy of the condensate for a given set of variational parameters is obtained from the energy functional

$$E(\boldsymbol{z}) = \left\langle \psi(\boldsymbol{r}, \boldsymbol{z}(t)) \middle| -\Delta + V_{\mathrm{ext}} + \frac{1}{2} V_{\mathrm{int}} \middle| \psi(\boldsymbol{r}, \boldsymbol{z}(t)) \right\rangle. \quad (7)$$

2. The variational ansatz

The dipolar BEC, described by the GPE (1) with the interaction potentials (2)–(3) and $s = 0$, naturally exhibits a cylindrical symmetry due to the alignment of the dipoles along the z-direction and due to the shape of the external trapping potential. In this case, the z-component of the angular momentum with eigenfunctions $\exp(\mathrm{i}m\phi)$ and the corresponding quantum number m are conserved. A suitable choice for the trial wave function is, therefore, given by the coupled Gaussians [22]

$$\psi(\boldsymbol{r}, \boldsymbol{z}(t)) = \sum_{i=1}^{N_g} \left(1 + \sum_{m \neq 0} \sum_{p=0,1} d^i_{m,p} \rho^{|m|} z^p \mathrm{e}^{\mathrm{i}m\phi} \right) \\ \times \exp\left(A^i_\rho \rho^2 + A^i_z z^2 + p^i_z z + \gamma^i \right) \quad (8)$$

with variational parameters $(d^i_{m,p}, A^i_\rho, A^i_z, p^i_z, \gamma^i)$. Here, the A^i_ρ, A^i_z describe the Gaussians' width in ρ- and z-direction, p^i_z the displacement of the BEC along the z-axis and the γ^i give the amplitude and phase of each Gaussian. Furthermore, the $d^i_{m,p}$ describe the non-axisymmetric contributions to the wave function with arbitrary angular momentum m and even ($p = 0$) or odd ($p = 1$) parity. We note that the ansatz

$$\psi(\boldsymbol{r}, \boldsymbol{z}(t)) = \sum_{i=1}^{N_g} \exp\left(A^i_x x^2 + A^i_y y^2 + A^i_z z^2 + \gamma^i \right) \quad (9)$$

with variational parameters $(A^i_x, A^i_y, A^i_z, \gamma^i)$ can be used as an alternative to Eq. (8), if only excitations with $m = 0$ ($A^i_x = A^i_y$) and $m = 2$ ($A^i_x \neq A^i_y$) rotational symmetry are of interest (see below).

Both the trial wave functions (8) and (9) have the advantage that all the integrals occurring in the equations of motion (6) and the mean-field energy (7) can be evaluated (semi-)analytically. For their calculation, we refer the reader to Refs. [22, 28] where they have been used in previous investigations.

C. Thermal decay rate

As we will discuss in Sec. III, the GPE (1) possesses – depending on the external physical parameters – one

ground state and several excited stationary states with different m-fold rotational symmetry. While the ground state is stable with respect to all local variations of the variational parameters, the excited states possess an unstable direction. Therefore the latter form saddle points of the energy functional (7) which have the physical meaning of "energy barriers". If the excitation energy of the BEC is larger than this barrier, it can be crossed along the unstable direction which results in the coherent collapse of the condensate as we will discuss below. In terms of reaction dynamics, each of the collectively excited states, therefore, forms a transition state (TS) on the way to the collapse of an excited BEC.

Having identified the TS, the corresponding reaction rate can be calculated by applying TST. This is possible after having performed a change of variables by means of a normal form expansion [29, 30] which maps the variational parameters to local canonical variables $(\boldsymbol{p}, \boldsymbol{q})$. In these the calculation of the flux over the saddle at an excitation energy larger than the saddle point energy is straightforward. Considering a condensate at an inverse temperature of $\beta = 1/k_{\mathrm{B}}T$, the respective reaction rates at different excitation energies have to be Boltzmann averaged, and within a harmonic approximation of the ground state and the saddle one obtains the result [31]

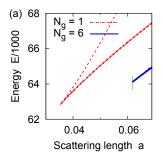$$\Gamma = \frac{1}{2\pi} \frac{\prod_{i=1}^{d} \omega_i}{\prod_{i=2}^{d} \omega'_i} \mathrm{e}^{-\beta E^\ddagger}. \qquad (10)$$

Here, the ω_i denote the stable oscillation frequencies in the vicinity of the ground state, ω'_i those at the excited state, and $E^\ddagger$ is the height of the energy barrier.

III. RESULTS

In this section, we present the results of our investigations of thermally excited dipolar BECs. We give a detailed discussion of the collectively excited states, point out the one which mediates the collapse, and calculate the corresponding collapse dynamics. We investigate the behavior of the energy barrier, and calculate the thermal decay rate for experimentally relevant temperatures.

Our main focus will be on the dependence of the different properties on the trap aspect ratio $\lambda = \gamma_z/\gamma_\rho$ and we therefore parameterize the external trapping parameters $\gamma_{\rho,z}$ by their mean value $\bar{\gamma} = (\gamma_\rho^2 \gamma_z)^{1/3}$. Our focus on the trap aspect ratio is because dipolar BECs exhibit the surprising feature that, for certain values of λ, they exhibit a blood-cell shaped ground state density distribution [8, 21]. In contrast to "conventional" density distributions where the maximum density of the atomic cloud is located in the center of the trap, such blood-cell shaped BECs show their maximum density away from the center.

We investigate both the regime with a conventional density distribution and the blood-cell-like regime, and as exemplary values for these regimes, we choose the trap
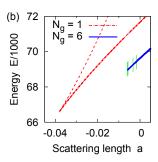
Figure 1. (Color online) Mean field energy E of the stationary states of a dipolar BEC for a mean trap frequency $\bar{\gamma} = 8000$ and a trap aspect ratio of $\lambda = 4$ (a) and $\lambda = 7$ (b). Shown are the values obtained from the simple variational ansatz using a single Gaussian wave function ($N_g = 1$) and the extended approach using the trial wave functions in Eqs. (8)–(9) ($N_g = 6$). The solid and dashed-dotted lines represent the ground state of the condensate and the dashed lines the collectively excited states. Using the simple variational ansatz, the energy difference between the ground and the excited state increases very rapidly while it is smaller than the linewidth of the plot within the extended approach. The vertical lines indicate the positions of the bifurcations (cf. Fig. 2).

aspect ratios $3 \leq \lambda \leq 4.5$ and $7 \leq \lambda \leq 8$. If not stated otherwise, the calculations presented in this section are performed using a number of $N_g = 6$ coupled Gaussians which have proven their capability to reproduce or even to exceed the results of numerical grid calculations [21].

A. Transition states of dipolar BECs

As we have mentioned above, the GPE possesses, in general, several stationary states which are fixed points ($\dot{z} = 0$) of the equations of motion (6). The existence of these states depends crucially on the physical parameters of the system, namely the external trapping parameters as well as the s-wave scattering length a which can be varied by means of Feshbach resonances in an experiment. Below a critical value a_{crit} the BEC cannot exist: From a physical point of view, the reason is that the attractive inter-particle interaction becomes so strong that it cannot be compensated anymore by the quantum pressure. Mathematically speaking, this is because the stable ground state of the condensate undergoes a bifurcation, in which it either becomes unstable or it vanishes completely.
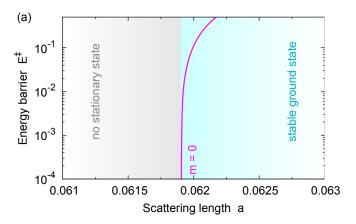
Figure 1 shows the stationary states of the dipolar BEC obtained from a single ($N_g = 1$) Gaussian trial wave function and $N_g = 6$ coupled wave functions in Eqs. (8)–(9). We choose a mean trap strength of $\bar{\gamma} = 8000$ and a trap aspect ratio of $\lambda = 4$ (conventional density distribution) as well as $\lambda = 7$ (blood-cell shaped BECs). Using a single Gaussian wave function (dashed-dotted and dashed

lines), the ground state and an excited state emerge in a tangent bifurcation at a scattering length of $a \approx 0.0353$ ($\lambda = 4$) and $a \approx -0.0382$ ($\lambda = 7$), respectively. The energy difference between the two states increases rapidly when the scattering length is increased.

Within the extended variational approach (solid line), both the value of the mean field energy and the position of the tangent bifurcation are shifted. Moreover, Rau et al. [21] and Kreibich et al. [22] showed that, for BECs with a biconcave shape, there is a whole cascade of stability changes of the condensate's ground state with respect to excitations with different m-fold rotational symmetry (the positions are indicated by the vertical bars in Fig. 1). Each of these is accompanied by with a bifurcation, in which two additional excited but unstable stationary states emerge. An important property of these states which have not yet been discussed in the literature is the fact that the energy difference with respect to the ground state is several orders of magnitude smaller than the one obtained from the simple variational ansatz. As we have already mentioned above, these excited states form transition states of the condensate's collapse dynamics, and because of the smaller energy barrier the corresponding reaction rates will be significantly higher than our calculations within the single Gaussian trial wave function [20] have predicted.

The essential property of the dipolar BEC concerning its thermally induced collapse is the height of the energy barrier $E^{\ddagger} = E_{\text{ex}} - E_{\text{gs}}$ because the reaction rate (10) depends exponentially on this quantity. Therefore, in the following we discuss the energy barriers in more detail. Fig. 2(a) shows the situation at a trap aspect ratio of $\lambda = 4$. Here the ground state of the BEC and an excited state which also has an axial symmetry ($m = 0$) emerge in a tangent bifurcation at a scattering length of $a_{\text{crit}} \approx 0.0619$ and the energy barrier $E^{\ddagger}$ between these states increases quickly by several orders of magnitude when the scattering length a is increased. Below the critical scattering length, there exists no state and above this value the $T = 0$ ground state is stable over the whole range of the scattering length. Other excited states with $m \neq 0$ do not participate in bifurcations together with the ground state.

The situation is different when we consider blood-cell shaped BECs at a trap aspect ratio of $\lambda = 7$ [see Fig. 2(b)]. Decreasing the scattering length from the region where a stable BEC exists the ground state becomes unstable with respect to elementary excitations with $m = 2$ rotational symmetry at a critical scattering length of $a_{\text{crit}} \approx -0.0016$. At the same point, an excited state bifurcates from the ground state which also exists at values $a > a_{\text{crit}}$. In contrast to the case $\lambda = 4$ where the ground state vanishes in a tangent bifurcation as discussed above, the ground state changes its stability in a pitchfork bifurcation at $\lambda = 7$ and persists as a stationary but unstable state also below this critical value. Due to the instability of all the states at $a < a_{\text{crit}}$, this region is, of course, not relevant for experiments. However, it is
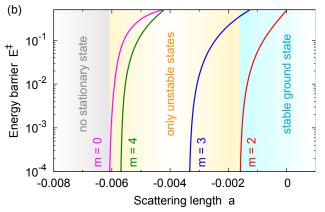
barrier.

Figure 2. (Color online) Energy barrier $E^{\ddagger} = E_{\text{ex}} - E_{\text{gs}}$ of a dipolar BEC for a mean trap frequency $\bar{\gamma} = 8000$ and a trap aspect ratio of $\lambda = 4$ (a) and $\lambda = 7$ (b). Both sub-figures show the region of the s-wave scattering length near the critical scattering length a_{crit}. For $\lambda = 4$ and a scattering length above the critical value ($a_{\text{crit}} \approx 0.0619$) there exist only the ground state of the BEC and a collectively excited state with $m = 0$ symmetry. For $\lambda = 7$ several collectively excited states with different symmetry $m = 0, 2, 3, 4$ are present. The one which is involved in the bifurcation at the critical scattering length ($a_{\text{crit}} \approx -0.0016$) is the $m = 2$ excited state and it is this state which has the smallest energy barrier in the parameter region where the BEC is stable. (See text for further explanations.)

relevant from a theoretical point of view, because other excited states which exist in the stable regime $a > a_{\text{crit}}$ can emerge there in further bifurcations. For the blood-cell shaped BEC in Fig. 2(b), three more bifurcations occur: At a scattering length of $a \approx -0.0033$ two excited states with $m = 3$ rotational symmetry bifurcate in a pitchfork bifurcation. Moreover, we observe the pitchfork bifurcation of two $m = 4$ states at $a \approx -0.0057$ and finally the tangent bifurcation together with an $m = 0$ excited state at $a \approx -0.0061$ below which no stationary state is present anymore. Note that all the energy barriers formed by the different excited states increase quickly by several orders of magnitude if the scattering length is increased from the respective bifurcation, and that it is the $m = 2$ state which corresponds to the smallest energy

B. Dynamics of excited BECs

The collectively excited states of the condensate discussed in the previous section correspond to saddle points of the energy functional (7) in the space of variational parameters, while the condensate's ground state corresponds to a local minimum. Because energy is conserved, we can discuss the physical meaning of the excited states in terms of the energy functional and with it interpret the possible dynamics. We first consider a BEC in its ground state. In this case, the dynamics resides at the minimum of the energy functional, and for slightly excited states the dynamics of the condensate is restricted to a small vicinity of the energy functional's minimum. A qualitative change in the dynamics of the BEC, however, occurs when the excitation energy of the condensate becomes larger than the energy of the lowest saddle in $\boldsymbol{z}$-space. In this case, a new region in the variational space becomes accessible and transitions between these regions correspond to crossings of the saddle point.

Because the physical meaning of the crossing of the saddle point is not clear a priori, we present the corresponding dynamics of the BEC in the following and consider a condensate which is excited to an energy slightly higher than the lowest saddle point energy. Figure 3 shows the corresponding dynamics for trap aspect ratios $\lambda = 4$ (a) and $\lambda = 7$ (b) in terms of the extensions $\sqrt{\langle x^2 \rangle}$ and $\sqrt{\langle y^2 \rangle}$ of the condensate (left-hand side) as well as in terms of the density profiles of the atomic cloud (right-hand side).

In the case of an excited BEC with conventional ground state density distribution at $\lambda = 4$ [see Fig. 3(a)] we observe at first collective oscillations of all the atoms (I). When the dynamics reaches the vicinity of the saddle, the motion turns into a quasi-stationary state (II) where the extension remains nearly constant for a period of time which is on the order of a few oscillation periods. At the end, the extension begins to shrink very rapidly (III) and it further contracts to zero extension (not shown) for $t \to 0$ which means the collapse of the BEC. Note that the dynamics is axisymmetric all the time ($\sqrt{\langle x^2 \rangle} = \sqrt{\langle y^2 \rangle}$), so that it is the breathing mode of the BEC which is associated with the crossing of the saddle, and the subsequent collapse. This behavior is to be expected since the only TS in this case has an $m = 0$ rotational symmetry [cf. Fig. 2(a)]. From the density profiles of the atomic cloud [see right-hand side of Fig. 3(a)], we see that the collective oscillations are associated with small density fluctuations of the BEC. At a certain time ($t = -0.00118$) the BEC reaches the "activated complex" with a critical density in its center that leads to the dominance of the attractive inter-particle interaction and to the subsequent collapse for $t \to 0$.

For a trap aspect ratio of $\lambda = 7$ [see Fig. 3(b)], we observe similar dynamics, also consisting of collective os-
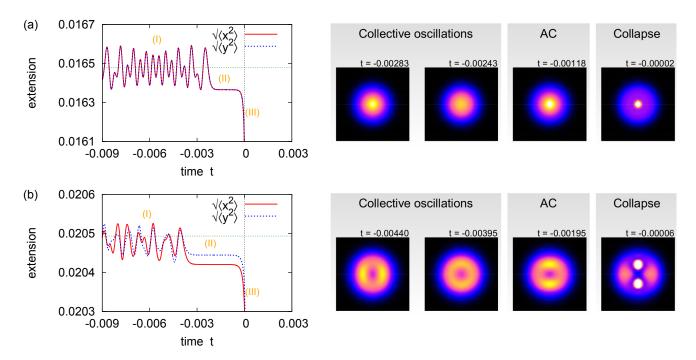
Figure 3. (Color online) Collapse dynamics of an excited dipolar BEC at (a) a trap aspect ratio $\lambda = 4$ and a scattering length of $a/a_d = 6.233 \times 10^{-2}$ as well as (b) $\lambda = 7$ and $a/a_d = 3.940 \times 10^{-4}$. Shown is the time evolution of the BEC's rms-extensions $\sqrt{\langle x^2 \rangle}$ and $\sqrt{\langle y^2 \rangle}$, respectively, and the excitation energy is slightly above the energy barrier which is $E^{\ddagger} = 1.0$ for both values of the scattering length given above. The dynamics shows (I) collective oscillations of the atomic cloud, (II) the formation of the quasi-stationary activated complex (AC) and (III) the collapse of the BEC.

cillations, crossing the saddle, and the collapse of the BEC. However, significant differences exist for blood-cell shaped BECs: At first, the dynamics is not axisymmetric which corresponds to the fact that the energetically lowest saddle has an $m = 2$ rotational symmetry [cf. Fig. 2(b)]. The oscillation mode which is responsible for the collapse is, therefore, the quadrupole mode. This behavior is astonishing, because the external trapping potential is axisymmetric, but it confirms hints for a symmetry breaking collapse scenario that we have obtained within a simple model in a previous investigation [20]. Secondly, we observe richer collapse dynamics as can be seen in the density profiles: The collective oscillations correspond to the dynamics where local density maxima occur on a ring around the center of the trap. Also the activated complex (reached at $t = -0.00195$) of the system is a density distribution which shows two local maxima on this ring. Precisely at these positions, the attractive interaction becomes dominant and the collapse of the BEC is now induced locally. Similar collapse dynamics also occur if one of the other saddles is crossed (not shown). According to the different rotational symmetry of the respective transition state, the whole collapse dynamics differs with respect to this point, meaning that a different number of angular patterns can be observed. However, independent of the respective rotational symmetry all these cases result in the collapse of the condensate, so that each of the states discussed above forms a barrier on the way to the BEC's collapse.

The collapse scenario shown in Fig. 3(b) is similar to the d-wave collapse investigated by Metz *et al.* [15], and also Wilson *et al.* [32] have investigated an angular collapse of dipolar BECs. We emphasize, however, that the physical situation in which this collapse is observed is totally different: In Refs. [15, 32] the stable $T = 0$ ground state of the BEC is considered and the collapse dynamics is investigated after having ramped down the s-wave scattering length below the critical value ($a < a_{\text{crit}}$), i.e. into a region where the condensate cannot exist anymore. By contrast, we observe similar dynamics in a region of the physical parameters where the BEC's ground state is stable, and there is also the quantitative difference that the collapse dynamics shown in Fig. 3 exhibit an $m = 2$ symmetry, whereas Wilson *et al.* observe an $m = 3$ collapse in their different experimental setup. The reason for the collapse of the BEC is in our case not a change of the physical parameters but the excitation of the condensate's internal degrees of freedom, namely its collective modes.
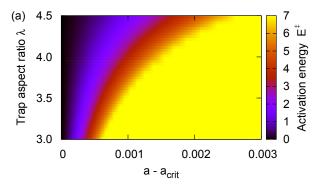
C. Activation energy and thermal decay rate

As discussed in Sec. III A, several TSs can exist which lead to different collapse scenarios with different rotational symmetry. To identify the one which is important for a BEC in an experiment we have to take into account the fact that a BEC in an experiment has a fi-

nite temperature $T > 0$. In contrast to the bosons in the quantum gas, the quasi-particles of the collective dynamics are not condensed and, therefore, all collective modes are populated according to the Boltzmann factor, and the corresponding reaction rates for each mode depend exponentially on the height of the respective energy barrier $E^{\ddagger}$ [cf. Eq. (10)]. Therefore, the mode which determines the decay rate of the condensate is always the one which corresponds to the saddle with the least energy because contributions from higher saddles are exponentially damped. At a trap aspect ratio of $\lambda = 4$ [Fig. 2(a)] this is the $m = 0$ excited state and for $\lambda = 7$ [Fig. 2(b)] it is the $m = 2$ state. The other excited states which exist for $\lambda = 7$ form barriers which lie several orders of magnitude higher, so that they can be neglected.

Figure 4 shows the behavior of the activation energy for two ranges of the trap aspect ratio $3 \le \lambda \le 4.5$ and $7 \le \lambda \le 8$. For a dipolar BEC with conventional density distribution we see in Fig. 4(a) that the behavior of the energy barrier significantly depends on the trap aspect ratio. For smaller trap aspect ratios $\lambda = 3$, we observe a rapid increase of the energy barrier when the scattering length is increased from the critical value and the energy barrier reaches a value of $E^{\ddagger} \approx 7$ already at $a - a_{\mathrm{crit}} = 0.0005$. At a larger trap aspect ratio $\lambda = 4.5$ the energy barrier increases much slower and reaches the same value only at a scattering length $a - a_{\mathrm{crit}} = 0.0025$, so that the relevant region is about five times larger. When we consider blood-cell shaped BECs [see Fig. 4(b)], there is only a minor change of the energy barrier's behavior when the trap aspect ratio is varied. However, the increase of the scattering length is even slower as compared to Fig. 4(a) and we reach a barrier height of $E^{\ddagger} \approx 7$ at a scattering length $a - a_{\mathrm{crit}} = 0.0045$ which is about nine times larger than at a trap aspect ratio of $\lambda = 3$.

This behavior of the energy barrier is of course directly reflected in the corresponding thermal decay rate of the dipolar BEC, shown in Fig. 5 for an inverse temperature of $\beta = 1$. We find the general behavior that there are very small decay rates $\Gamma \lesssim 1$ far away from the critical scattering length which correspond to lifetimes of several seconds. In this parameter region, the process investigated in this paper is, therefore, not relevant and other processes limit the lifetime of the condensate. However, when the scattering length is decreased the decay rate increases significantly by several orders of magnitude and reaches up to $\Gamma \gtrsim 10^3$. Furthermore, for blood-cell shaped BECs we identify a region of an enhanced decay rate at $a - a_{\mathrm{crit}} = 0.002 - 0.003$. This behavior is caused by the eigenfrequencies of the oscillation modes forming the prefactor in Eq. (10): Here, several stable eigenfrequencies of the excited state drop down in the same parameter region. The physical interpretation of this behavior is that the region where transitions take place in the vicinity of the transition state becomes broader, so that the flux over the saddle and hence the decay rate increases.
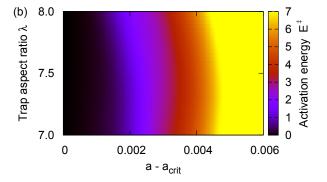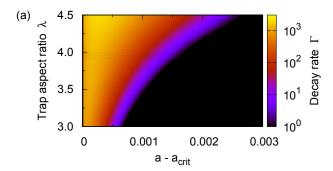

Figure 4. (Color online) Activation energy $E^{\ddagger}$ for the thermally induced coherent collapse for (a) non-blood-cell shaped BECs at trap aspect ratios $3 \le \lambda \le 4.5$ and (b) blood-cell shaped BECs at $7 \le \lambda \le 8$. In (a) the energy barrier with increasing scattering length becomes smaller the higher the trap aspect ratio is. For blood-cell shaped BECs (b) the behavior of the energy barrier with increasing scattering length changes only marginally when varying the trap aspect ratio. We note that, for a ^{52}Cr condensate consisting of $N = 10\,000$ bosons, the range of the energy barrier shown ($0 \le E^{\ddagger} \le 7$) corresponds to a thermal energy $T = E^{\ddagger}/k_{\mathrm{B}}$ of $0 \le T \le 141\,\mathrm{nK}$ which is about 20% of the critical temperature ($T_{\mathrm{c}} = 700\,\mathrm{nK}$ [1]). The range of the scattering length is 0.275 Bohr radii above the critical scattering length in (a) and 0.55 Bohr radii in (b).

1. The temperature regime investigated and the influence of the strength of the DDI

Dipolar BECs have first been realized with ^{52}Cr atoms [1] which possess a magnetic moment of $\mu = 6\mu_{\mathrm{B}}$ (μ_{B} is the Bohr magneton). For an exemplary chromium BEC consisting of $10\,000$ bosons, the range of the scattering length shown in Fig. 4 is 0.55 Bohr radii and the energy barrier $0 \le E^{\ddagger} \le 7$ corresponds to a thermal energy $T = E^{\ddagger}/k_{\mathrm{B}}$ of $0 \le T \le 141\,\mathrm{nK}$ which is about 20% of the critical temperature ($T_{\mathrm{c}} = 700\,\mathrm{nK}$ [1]). The temperature used in Fig. 5 is $20\,\mathrm{nK}$ and the range of the decay rate $1 \le \Gamma \le 3 \times 10^3$ corresponds to mean lifetimes $\tau = \Gamma^{-1}$
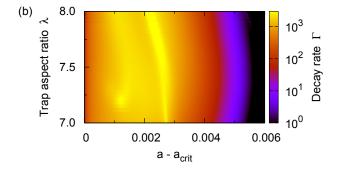
Figure 5. (Color online) Decay rate due to the thermally induced collapse for (a) non-blood-cell shaped BECs at $3 \leq \lambda \leq 4.5$ and (b) blood-cell shaped BECs at $7 \leq \lambda \leq 8$ at an inverse temperature of $\beta = 1$. Depending on the trap aspect ratio, the decay rate shows a similar behavior as the activation energy in Fig. 4. The ranges of the trap aspect ratios and the scattering length are the same as in Fig. 4 and the range of the decay rate ($1 \leq \Gamma \leq 3 \times 10^3$) corresponds to mean lifetimes $\tau = \Gamma^{-1}$ of $1.3\,\mathrm{ms} \leq \tau \leq 3800\,\mathrm{ms}$ for a ^{52}Cr BEC of $N = 10\,000$ atoms. The inverse temperature $\beta = 1$ corresponds to $T = 20\,\mathrm{nK}$.

of $1.3\,\mathrm{ms} \leq \tau \leq 3800\,\mathrm{ms}$ for such a condensate, meaning that the lifetime of the BEC is reduced to a few milliseconds in the vicinity of the critical scattering length.

These parameters also show that the investigation of the BEC within the GPE is justified: The frequency of the respective quasi-particle mode which is responsible for the induced collapse shrinks to zero when the critical scattering length is approached. Very close to this value, it is, therefore, small and we calculate values of a few hundred to a few thousand oscillations per unit time (in particle number scaled units) close to the critical scattering length a_crit. For the example given, these correspond to values $26.4\,\mathrm{s}^{-1} \leq \omega \leq 264\,\mathrm{s}^{-1}$. Furthermore, the temperature scale on which the thermal activation of the quasi-particle modes has to be expected, can be estimated when one assigns to each oscillation mode an energy of $E = \hbar\omega$ and the corresponding temperature $T = E/k_\mathrm{B}$. This yields the temperature regime $0.2\,\mathrm{nK} \leq T = \hbar\omega/k_\mathrm{B} \leq 2\,\mathrm{nK}$. On the other hand, single-

particle excitations can occur due to the thermal energy. Although modifications are caused by the inter-particle interactions, their contribution can be roughly estimated using the condensate fraction of a ideal Bose gas in a harmonic trap, $N/N_0 = 1 - (T/T_c)^3$. The temperature regime in Fig. 5 is $0 \leq T \leq 20\,\mathrm{nK}$, so that the non-condensate fraction is less than 2.5×10^{-5}. Single-particle excitations can, therefore, be neglected and the condensate can be well described by the GPE.

Dipolar BECs are also accessible with ^{164}Dy ($\mu = 10\mu_\mathrm{B}$) and ^{168}Er ($\mu = 7\mu_\mathrm{B}$) atoms [2, 3]. Because of their larger magnetic moment and their higher masses, the corresponding "dipole length" a_d (see Sec. II A) is significantly larger than that of ^{52}Cr. Calculating the respective values, we obtain that it is increased by a factor of about 8.8 for ^{164}Dy and 4.4 for ^{168}Er. For these elements we, therefore, expect even larger effects. On the one hand, this is because the range of the s-wave scattering length in which the process presented in this paper is relevant, becomes larger by this factor. For example the range of the scattering length in Figs. 4(b) and 5(b) becomes 2.40 Bohr radii in case of erbium and 4.78 Bohr radii in case of dysprosium. On the other hand, the dipolar energy scales as $E_\mathrm{d} \sim a_\mathrm{d}^{-2}$. Consequently, the energy barriers discussed above are by a factor of $1/(8.8)^2 \approx 0.0129$ smaller for dysprosium and $1/(4.4)^2 \approx 0.0517$ times smaller for erbium. Consequently, the thermal decay rates are increased significantly for these elements.

2. Stability threshold at finite temperatures

The fact that a condensate at finite temperature is unstable with respect to a coherent collapse and has a significantly shortened lifetime in the vicinity of the critical scattering length needs to be considered when one investigates the stability threshold of the condensate. From a theoretical point of view this threshold is determined by a stability analysis of the $T = 0$ ground state with respect to elementary excitations. Within numerical approaches to the GPE this can be performed using the Bogoliubov-de Gennes equations, or in terms of variational approaches the same is given by the eigenvalues of the Jacobian matrix of the equations of motion at the fixed points. (In case of the variational approach, the $T = 0$ stability threshold is given by the highest-lying bifurcation of the ground state.) In experiments, the stability threshold can be determined by successively decreasing the s-wave scattering length to a certain value and testing whether or not the BEC still exists there.

However, from our calculations we expect that these theoretical and experimental methods will, in general, lead to different results due to the finite temperature of the BEC in an experiment. As our investigations show, the lifetime of the BEC at $T > 0$ is significantly reduced in the vicinity of the critical scattering length and it can decay in a parameter region where the $T = 0$ ground state

is stable. Thus, when one decreases the scattering length, the condensate decays because of the thermally induced collapse before the critical value has been reached. As a consequence, we expect that the experimentally measured values of the stability threshold should be larger than predicted from the theory at $T = 0$. The deviation will depend on the temperature of the BEC and, for typical values of several ten nK, it has to be expected to be on the order of a few Bohr radii.

This interpretation can be an explanation of the measurements performed by Koch *et al.* [10] who have observed such a behavior for a wide range of the trap aspect ratio λ in dipolar BECs. Similar observations have also been made in BECs without long-range interaction [33].

IV. CONCLUSION

In this paper, we have investigated dipolar BECs at finite temperature within an extended variational framework. We have shown that the excitation of collective oscillations can induce the coherent collapse of the condensate in a regime of the external physical parameters where the $T = 0$ ground state is stable. Our investigations reveal that there exist – depending on the trapping parameters and the s-wave scattering length – several transition states with different rotational symmetry which can mediate collapse dynamics of the BEC.

For BECs at finite temperature, we identified the $m = 0$ collectively excited stationary state to mediate the collapse of dipolar BECs with conventional density distribution, and the $m = 2$ state in the case of a blood-cell shaped BEC. The corresponding collapse dynamics shows qualitative differences: In the first case we observe a global collapse, while in the second case the BEC collapses locally with a d-wave symmetry.

The activation energy necessary to induce the collapse shows a significant dependence on the trap aspect ratio of the confining trap. Depending on the strength of the dipolar interaction its magnitude is relevant for experiments with scattering lengths up to several Bohr radii above the critical scattering length. In this region the lifetime of the condensate can be significantly reduced to the order of a ms. This means that it is experimentally demanding to reach this regime.

Because of the gradually decreasing energy barriers the process discussed in this paper becomes more and more important when one approaches the critical scattering length, so that the temperature of the gas can have a direct influence on the experimentally measured value of the stability threshold.
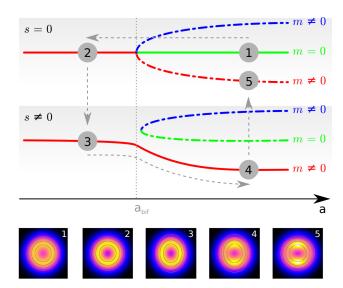
Figure 6. (Color online) Schematic description of the procedure to systematically access collectively excited stationary states which bifurcate from the ground state. Shown is the typical bifurcation scenario between the ground state and the excited states with m-fold rotational symmetry. The solid lines depict the states which cross the bifurcation smoothly, and the dashed lines represent the emerging states. The numbers indicate the single steps of the procedure described in the text. (Top) In an axisymmetric trap [$s = 0$ in Eq. (2)] the ground state with $m = 0$ passes the bifurcation smoothly and the $m \neq 0$ states bifurcate at a certain value a_{bif} of the s-wave scattering length. (Center) The bifurcation scenario changes when the rotational symmetry of the external trap is changed ($s \neq 0$) in a way that the state which crosses the bifurcation smoothly has an $m \neq 0$ rotational symmetry. (Bottom) The density profiles show the behavior of the wave function during the steps 1–5 exemplarily for the $m = 2$ bifurcation. The shape of the external trap is indicated by the contours.

Appendix: Systematic access to excited states

Provided that the ground state of the condensate is known, there is a systematic way to access the excited states: Therefore, we generalize a method from Gutöhrlein *et al.* [34] which is based on the following facts: On the one hand, the excited states bifurcate from the ground state at certain values of the s-wave scattering length a so that the participating states merge at the bifurcations. One the other hand, the state which goes through the bifurcation smoothly can be chosen by the rotational symmetry of the external trap.

In case of an axisymmetric trapping potential [$s = 0$ in Eq. (2)], the ground state of the BEC also exhibits this symmetry. Assume that this ground state changes its stability with regard to elementary excitations with rotational symmetry $m \neq 0$ at a certain scattering length

a_{bif}, then there exist two excited states which bifurcate from the ground state in a pitchfork bifurcation. In an axisymmetric trap, these states are physically equivalent because they only differ by a rotation of the condensate and they can be accessed as demonstrated in Fig. 6: Starting point is the ground state of the axisymmetric trap ($s = 0$) at a value of the scattering length above a_{bif} (position 1) and we want to access the excited state with $m \neq 0$ at the same value of the scattering length (position 5). In a first step, we change the scattering length to the "other side" of the bifurcation (position 2) and in a second step the trap symmetry is broken by adiabatically increasing the parameter s to a sufficiently large value $s > 0$ (position 3). Here, the rotational symme-

try m of the trap has to be chosen according to the value which changes its stability at a_{bif} so that the ground state naturally adopts this rotational symmetry. In the third step, the scattering length is increased to a value above the bifurcation (position 4) which retains the rotational symmetry and, finally, the external trap is again changed back adiabatically to an axisymmetric shape ($s = 0$). The result at position 5 is the collectively excited state with the m-fold rotational symmetry and with this procedure, we are able to access excited states with arbitrary $m \neq 0$ bifurcating from the ground state. In addition, the $m = 0$ excited state can be found by randomly varying the variational parameters in the vicinity of the bifurcation in a way that the wave function keeps its axial symmetry.

[1] A. Griesmaier, J. Werner, S. Hensler, J. Stuhler, and T. Pfau, Phys. Rev. Lett. **94**, 160401 (2005)
[2] M. Lu, N. Q. Burdick, S. H. Youn, and B. L. Lev, Phys. Rev. Lett. **107**, 190401 (2011)
[3] K. Aikawa, A. Frisch, M. Mark, S. Baier, A. Rietzler, R. Grimm, and F. Ferlaino, Phys. Rev. Lett. **108**, 210401 (2012)
[4] P. Pedri and L. Santos, Phys. Rev. Lett. **95**, 200404 (2005)
[5] R. Nath, P. Pedri, and L. Santos, Phys. Rev. Lett. **102**, 050401 (2009)
[6] I. Tikhonenkov, B. A. Malomed, and A. Vardi, Phys. Rev. Lett. **100**, 090406 (2008)
[7] O. Dutta and P. Meystre, Phys. Rev. A **75**, 053604 (2007)
[8] S. Ronen, D. C. E. Bortolotti, and J. L. Bohn, Phys. Rev. Lett. **98**, 030406 (2007)
[9] K. Góral, K. Rzazewski, and T. Pfau, Phys. Rev. A **61**, 051601 (2000)
[10] T. Koch, T. Lahaye, J. Metz, B. Fröhlich, A. Griesmaier, and T. Pfau, Nature Physics **4**, 218 (2008)
[11] L. Santos, G. V. Shlyapnikov, P. Zoller, and M. Lewenstein, Phys. Rev. Lett. **85**, 1791 (2000)
[12] K. Góral and L. Santos, Phys. Rev. A **66**, 023613 (2002)
[13] L. Santos, G. V. Shlyapnikov, and M. Lewenstein, Phys. Rev. Lett. **90**, 250403 (2003)
[14] R. M. Wilson, S. Ronen, J. L. Bohn, and H. Pu, Phys. Rev. Lett. **100**, 245302 (2008)
[15] J. Metz, T. Lahaye, B. Fröhlich, A. Griesmaier, T. Pfau, H. Saito, Y. Kawaguchi, and M. Ueda, New J. Phys. **11**, 055032 (2009)
[16] T. Lahaye, J. Metz, B. Fröhlich, T. Koch, M. Meister, A. Griesmaier, T. Pfau, H. Saito, Y. Kawaguchi, and M. Ueda, Phys. Rev. Lett. **101**, 080401 (2008)
[17] S. Hensler, J. Werner, A. Griesmaier, P. O. Schmidt, A. Görlitz, T. Pfau, K. Rzazewski, and S. Giovanazzi, Appl. Phys. B **77** (2003)
[18] H. T. C. Stoof, Journal of Statistical Physics **87**, 1353 (1997)
[19] K. Marquardt, P. Wieland, R. Häfner, H. Cartarius, J. Main, and G. Wunner, Phys. Rev. A **86**, 063629 (2012)
[20] A. Junginger, J. Main, G. Wunner, and T. Bartsch, Phys. Rev. A **86**, 023632 (2012)
[21] S. Rau, J. Main, H. Cartarius, P. Köberle, and G. Wunner, Phys. Rev. A **82**, 023611 (2010)
[22] M. Kreibich, J. Main, and G. Wunner, J. Phys. B: At. Mol. Opt. Phys. **46**, 045302 (2013)
[23] N. P. Proukakis and K. Burnett, J. Res. Natl. Inst. Stand. Technol. **101**, 457 (1996)
[24] A. Griffin, Phys. Rev. B **53**, 9341 (1996)
[25] P. B. Blackie, A. S. Bradley, M. J. Davis, R. J. Ballagh, and C. W. Gardiner, Adv. Phys. **57**, 636 (2008)
[26] A. D. McLachlan, Molecular Physics **8**, 39 (1964)
[27] H. Cartarius, T. Fabčič, J. Main, and G. Wunner, Phys. Rev. A **78**, 013615 (2008)
[28] S. Rau, J. Main, and G. Wunner, Phys. Rev. A **82**, 023610 (2010)
[29] A. Junginger, J. Main, G. Wunner, and M. Dorwarth, J. Phys. A: Math. Theor. **45**, 155201 (2012)
[30] A. Junginger, M. Dorwarth, J. Main, and G. Wunner, J. Phys. A: Math. Theor. **45**, 155202 (2012)
[31] P. Hänggi, P. Talkner, and M. Borkovec, Rev. Mod. Phys. **62**, 251 (1990)
[32] R. M. Wilson, S. Ronen, and J. L. Bohn, Phys. Rev. A **80**, 023614 (2009)
[33] J. L. Roberts, N. R. Claussen, S. L. Cornish, E. A. Donley, E. A. Cornell, and C. E. Wieman, Phys. Rev. Lett. **86**, 4211 (2001)
[34] R. Gutöhrlein, J. Main, H. Cartarius, and G. Wunner, J. Phys. A **46**, 305001 (2013)